Earth Surface Processes and Landforms
Earth Surf. Process. Landforms **23,** 1123–1134 (1998)

NUMERICAL ANALYSIS OF COASTAL CLIFF FAILURE ALONG THE PEMBROKESHIRE COAST NATIONAL PARK, WALES, UK

P. DAVIES[1], A. T. WILLIAMS[1]* AND P. BOMBOE[2]

[1] *Faculty of Applied Sciences, Bath Spa University College, Newton Park, Bath, UK*
[2] *Geological Engineering Department, Faculty of Geology and Geophysics, University of Bucharest, Romania*

Received 1 July 1996; Revised 1 August 1998; Accepted 28 August 1998

ABSTRACT

Cliff stability within the Pembrokeshire Coast National Park was evaluated using a numerical model applied at four sites representative of rock mass failure phenomena and major sedimentary geological sequences. The sites were: Mill Bay, (Old Red Sandstone); St Govan's Head, Carboniferous Limestone (Dinantian); Druidston, Millstone Grit (Namurian) and Lower Coal Measures (Westphalian); and Wiseman's Bridge, Lower Coal Measures (Westphalian). The study integrated a range of geotechnical parameters, measured in the field and laboratory, into a model to predict the likely failure mechanisms. The model is based on the existence of rock prisms delineated by structural parameters, i.e. joints, bedding planes and critical tension fractures behind the cliff face. An iterative approach is used to define the dip of the most probable, stepped failure surface at the base of any potentially unstable multiblock system and to calculate the sliding and toppling forces for each block in the cliff mass. Prediction compared favourably with field observations at three of the four selected sites, i.e. Druidston, St Govan's Head and Wiseman's Bridge. At Druidston sliding is predicted and dominates in the basal blocks, whilst toppling is confined to the upper cliff and is dependent on movement of the lower structural units. St Govan's Head is shown to have a low risk of toppling and sliding and this was predicted except where basal undercutting reaches a depth of 1·0m or lateral forces exceed 100 kN m^{-2} when failure could occur. © 1998 John Wiley & Sons, Ltd.

KEY WORDS coastal cliff failure; Pembrokeshire Coast National Park; numerical analyses

INTRODUCTION

The coastal cliffs are characterized by recession and abundant superficial failures within a wide range of rock and structural environments of the Pembrokeshire Coast National Park (PCNP). At a general level, cartographic measurements using the 1907 and 1973 Ordnance Survey 1:2500 maps and based on the identified cliff line, mean high water mark (MHWM) and mean low water mark (MLWM) can be used to identify average coastal cliff recession rates for a variety of wave energy and geological settings. For example, based on sampling 100m interval map information, MHWM recession rates range from 18·0–40·0 cm a^{-1} for sites within the Lower Coal Measures of St Brides Bay to as low as 1·0 cm a^{-1} for Carboniferous Limestone sections around St Govan's Head. The cartographic survey results for MLWM and cliff line recession show similar characteristics and there is a considerable variation at individual sites using the different base line datum points, e.g. in the Lower Coal Measures west of Wiseman's Bridge the recession rates vary from 68·1 cm a^{-1} (MLWM) to 14·5 cm a^{-1} (MHWM) and 3·1 cm a^{-1} (cliff line). The accuracy of cartographic data is suspect, however, and as Carr (1962, p. 114) noted, 'most topographic maps show traces of bad survey'. Further elucidation of the reasons for such wide-ranging spatial contrasts in recession would require a level of site survey, wave energy and geological information logistically beyond that available for the present analysis. However, coastal cliff failure is a serious problem at specific sites within the PCNP and has adversely affected utilization of the coastal footpath. Consequently, the aim of this study is to develop a numerical model analysing the nature of cliff instability within the area with a view to predicting the likely failure mode at particular sites. Locations were selected covering an array of cliff morphologies, wave climates and containing

* Correspondence to: Professor A. T. Williams, Geography Department, Faculty of Applied Sciences, Bath Spa University College, Newton Park, Bath, UK

CCC 0197-9337/98/121123–12 $17.50

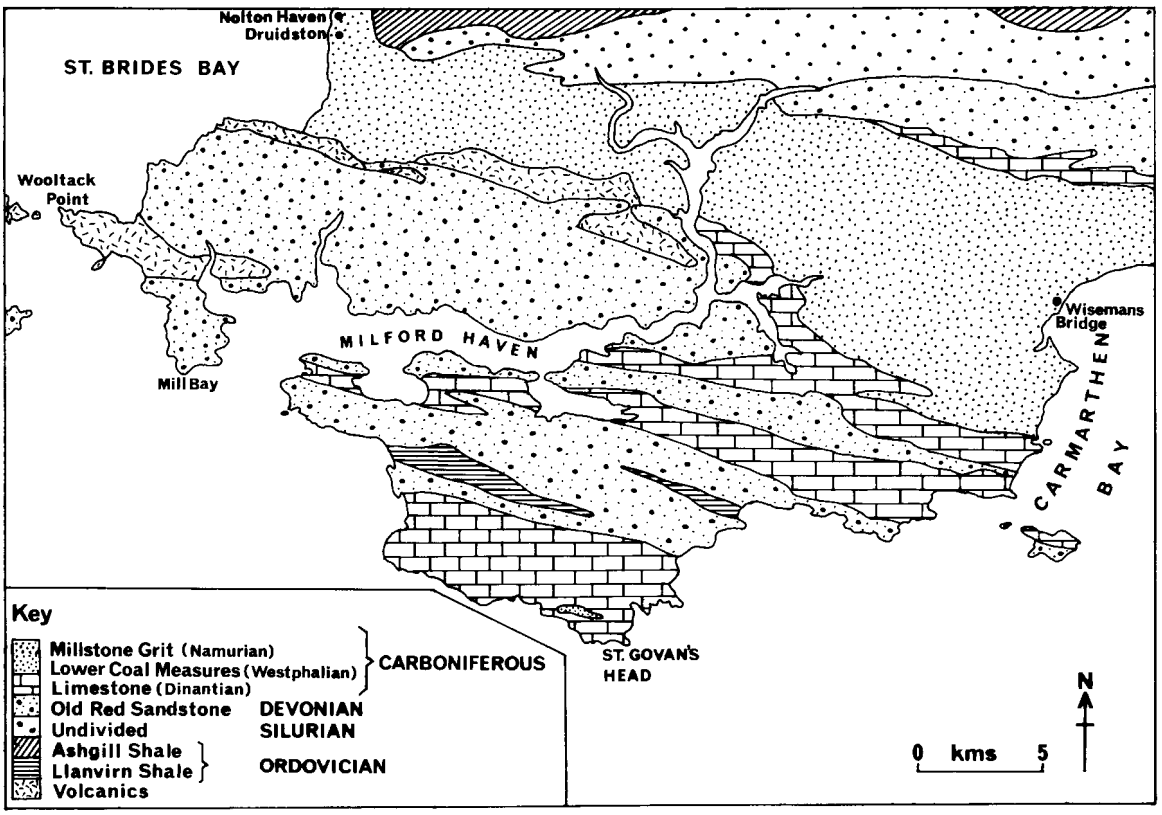

Figure 1. Location and geological map of investigated sites: Druidston, St Govan's, Mill Bay and Wisemans Bridge

abundant and representative failure types for the broad geological divisions of this environment. In addition, sites had to be accessible under the prevailing sea state conditions since more than 70 per cent of the basal areas of the coastal cliffs are under water at low tide conditions. Four sites were finally selected: Mill Bay (Old Red Sandstone); St Govan's Head, Carboniferous Limestone (Dinantian); Druidston, Millstone Grit (Namurian) and Lower Coal Measures (Westphalian); and Wiseman's Bridge, Lower Coal Measures (Westphalian). All sites (Figure 1) were intensively studied and measurements were taken in the field and laboratory of geological and geotechnical parameters for inclusion within the numerical model.

GEOLOGICAL BACKGROUND

The PCNP is of outstanding geological interest and beauty. The coastal sections, extending a distance of 272 km, expose rocks ranging in age from Precambrian to late Carboniferous. Four typical sites were selected for analyses of engineering geology properties and failure mechanisms. The sites were chosen to represent typical geological environments for Carboniferous Coal Measures, Carboniferous Limestone and Old Red Sandstone (Figure 1 and Table I). At Druidston, the Namurian and Westphalian rocks, consisting of massive coarse-grained sandstones overlying sandstone/shale/clay beds, are faulted against Ordovician slates. At St Govan's Head, shelly Carboniferous Limestone is exposed and faulting often occurs in reticulate patterns, two large thrust faults dominating the location. At Mill Bay, a thick series of Old Red Sandstone outcrops occur. At Wiseman's Bridge, along the inner sheltered shores of Carmarthen Bay, sandstones and shales of the Lower Coal Measures outcrop in a series of fault blocks.

Table I. Geological parameters associated with investigated rock types

Location	Druidston		St Govan's Head		Mill Bay		Wiseman's Bridge	
Movement volume	1250 m^3		60 m^3		30 m^3		28 m^3	
Geological group	Millstone Grit (Namurian); Lower Coal Measures (Westphalian)		Carboniferous Limestone (Dinantian)		Old Red Sandstone		Lower Coal Measures (Westphalian)	
Rock type	Silty sandstones and shale		Limestone		Sandstone		Sandstone/ siltstone/ shale/clay	
Strike/dip	165–345°/57°		140–320°/85°		115–295°/85°0		135–315°/80°	
Discontinuities	**Horizontal**	**Vertical**	**Horizontal**	**Vertical**	**Horizontal**	**Vertical**	**Horizontal**	**Vertical**
Strike/dip	153–333°/22°	30–210°/85°	95–275°/10°	140–320°/90°	20–200°/15°	55–235°/70°	90–270°/15°	100–280°/80°
Joint spacing	200–250 mm	150-200 mm	1·5–2 m	1–1·5 m	30–60 mm	400–800 mm	250–400 mm	600–800 mm
Extent	> 1 m	< 200 mm	> 5 m	> 5 m	3–5 mm	5–10 mm	> 5 m	> 5 m
Width of joints	10–15 mm	1–5 mm	3–5 mm	5–10 mm	> 1 m	< 0·5 m	2–10 mm	2–10 mm

MARINE INFLUENCES

Waves are the dominant force modifying coastlines (Komar, 1976). The PCNP is located in the southern section of the partly enclosed Irish Sea Basin where westerly air flow dominates. Published data on wave climate parameters are lacking but unpublished IOS data indicates maximum wave heights of 10–12 m for a 50 year return interval, whilst Jones' (1987) analysis of the Aberporth, Cardigan Bay, wave rider buoy data suggests a higher value of 15m. Storm wave energy values using the Sverdrup, Munk, Bretschneider technique and meteorological data for the period 1971 to 1985 are shown to have a mean value of 16 225 $Jm^{-1} s^{-1}$ for 33 storm events with a maximum of 38 439 $Jm^{-1} s^{-1}$. Whilst this information gives a general indication of wave power, the wave environment is complex and difficult to measure. Basal erosion by waves has an important influence on coastal cliff instability and Sunamura (pers. comm.) has stressed that even though the assailing wave force (F_w) is recognized as important to a full understanding of cliff face behaviour it has not yet proved possible to determine an index which accurately represents field conditions of this force. In addition, as Sunamura (1992) describes, there are further temporal variations in F_w due to the size and amount of debris entrapped in waves and, as yet, this component has also proved impossible to quantify and evaluate in the field with respect to cliff failure. Because of these difficulties, a detailed study of F_w does not form part of the numerical analysis of failure mode carried out within this paper. This does not, however, invalidate the modelling of basal notching, geotechnical parameters and within-cliff mechanisms of failure undertaken in the study.

FAILURE MODES

Sunamura (1992) has described the four primary types of failure on rocky coasts: falls, topples, slides and flows. They are mainly dependent upon lithological variation, structure and geotechnical properties. Predetermined natural rock discontinuities and planes of weakness are of prime importance in rock slope failure (Jumikis, 1983). Falls, topples and slides occur in the study area. Falls occur where steeply sloping rock masses are composed of well-jointed rock. They move mainly through the air and have been studied in the field and theoretically by evaluation of the rock trajectory. Coastal examples of falls have been analysed by Williams and Davies (1987) in the gently dipping, steeply jointed Lower Lias limestones of south Wales, and by Jones and Williams (1991) in the Aberystwyth Grits of west Wales.

Topples involve rotation of a block around a fulcrum and the free fall element is limited. Numerical analyses by Davies *et al.* (1991) and Williams *et al.* (1993) in the *bucklandi* and *angulata* horizons of the

Lower Lias of south Wales demonstrated the importance of joint inclination, tension fracture development and basal undercutting in the generation of toppling failure. At sites with a cliff overhang toppling was found to develop even under conditions of low critical thrust forces, e.g. associated with expansion of joint infill clays and saturation of joints with storm wave water.

Slides are a widely occurring failure type and involve block movement along a distinct failure surface. They may be classified as planar or rotational in character depending on the shape of the failure surface. A model of sliding failure has been developed by Taylor (1948) and Carson (1971) for plane failure along linear surfaces. It involves assessment of the balance between shear stresses and shear strength on the failure plane and suggests that the same slope angle appears repeatedly as the cliff recedes. In areas of high rock resistance, sliding may only be induced by the increase in shear stresses associated with basal wave notching. Hutchinson (1972), in a study of chalk cliff failure in the Isle of Thanet in southern England, showed that at the time of collapse a tension fracture had developed to a depth of almost half the 15 m cliff height and the wave notch had penetrated to a depth of 0.5 m. Williams *et al.* (1993) similarly showed the significance of tension fracture characteristics and basal notching. In their study of the Lias in south Wales, it was shown that the failure may involve toppling as well as stepped failure path sliding as the ratio of undercutting depth to tension fracture distance from the cliff face increased.

GEOTECHNICAL PARAMETERS

Terzaghi (1962), Hoek and Bray (1981) and others have outlined the multiplicity of factors influencing rock slope stability, including gravitational, geomorphological, lithological, structural, hydrological, climatological and anthropogenic phenomena. This paper attempts to relate failure mechanisms to geotechnical parameters.

Hoek and Bray (1981) have demonstrated the importance of orientation and density of rock discontinuities, the latter being a collective term covering bedding planes, laminations, joints and faults. Where major open discontinuities exist, deformation occurs along these rather than through breakdown of the intact rock. Scoble and Leigh (1982) indicated that the steepest angle at which a slope remains stable depends largely upon the orientation of the discontinuities relative to the slope, supporting Terzaghi's (1962) conclusion. The key discontinuity measures monitored in the present study were orientation, spacing, persistence, roughness, wall strength, aperture, filling, seepage, number of joint sets and block size using the ISRM (1981) methodology.

The laboratory testing equipment employed was an ESH 2000KN machine for measuring confined triaxial and unconfined uniaxial compressive strength of the major rock types of the PCNP using BX-sized core specimens, where possible, in conjunction with Hoek and Brown's (1988) and Hoek's (1990) guideline equations. In the field, uniaxial compressive stength was assessed with a Schmidt hammer ('L' type) using the methodologies and corrections of Miller (1965), Day and Goudie (1977) and Kazi and Al-Mansom (1980). Hoek and Bray (1981) demonstrated the problems of determining shear strength in rocks showing micro- and meso-scale fracturing and weathering. Patton (1966) has also shown that the degree of discontinuity waviness has to be taken into account in the shear strength formula, i.e.

$$\tau = \sigma_\eta \tan\,(\phi + i)$$

where τ = shear strength, σ_η = the effective normal stress, i = the angle between the peaks of first-order projections and the mean plane of shearing, and ϕ = the angle of shear by friction and through the asperities.

Barton (1973) demonstrated that compressive and tensile strengths of rocks decline with increasing moisture content, whilst Barton and Choubey's (1977) equation summarizes the complexity of assessing the shear strength of rock masses with discontinuities:

$$\tau = \tan[JRC \log_{10}\,(JCS/\sigma_\eta) + \phi_b]$$

where JRC = joint roughness coefficient, JCS = joint compressive strength, ϕ_b = the basic friction angle and σ_η = the effective normal stress.

Bandis *et al.* (1981) indicated that both JCS and JRC reduce with increasing joint size. JRC values were estimated in the field and measured in the laboratory from tilt tests on rock samples with fresh natural discontinuities and calculated using the following equation:

$$JRC = \alpha - \phi_r / \log_{10}(JCS/\sigma_\eta)$$

where α = the tilting angle at failure and ϕ_r = the residual angle of friction along a joint.

The residual friction angle (ϕ_r) was obtained from this data using the empirical relationship:

$$\phi_r = (\phi_b - 20^0) + 20(r/R)$$

where r = the Schmidt hammer rebound value on the weathered joint surface and R = the rebound value on the unweathered joint surface.

THE NUMERICAL MODEL

Twelve parameters were measured in the field and laboratory: cliff height, cliff face angle, dip, strata thickness, joint plane friction angle, joint spacing, joint length, unit weight, friction angle, strike azimuth, compressive strength and tensile strength.

Numerical modelling follows the approaches developed by Davies *et al.* (1991) and Williams *et al.* (1993) which were successfully applied to sedimentary sequences of the lower Lias rocks of the Glamorgan Heritage Coast, UK. It is based on the existence of rock prisms which can be delineated by a range of structural parameters including the average spacing of the major joints (λ_s), average spacing of the bedding planes (λ_m), dip angle of the bedding planes (α), dip angle of the major joints (τ) and the existence of tension fractures of varying depths (Z) behind the cliff face. These are used to define the dip angle of the most probable stepped failure surface at the base of any potentially unstable multiblock system in the cliff mass (Figure 2). It is assumed that the tension fracture propagates in the direction of largest stress release and that negligible resistance is developed along the lateral boundaries of the block at failure.

Using Hoek and Bray's (1981) equations, the critical tension fracture depth (z) can be calculated from:

$$z = H[1 - \sqrt{(\cot \omega \cot \beta)}]$$

where H = height of the cliff face, ω = the cliff face angle and β = dip of the average slip surface. The tension fracture distance from the cliff edge is accurately measured in the field or is estimated from average spacing between continuous master joints parallel to the cliff face.

The shape of the sliding surface and its position are invariably uncertain but the simulation programme is capable of determining the average dip angle (β) of the translation failure path by iterative techniques if the average dip of the bedding planes (α), the joint spacing (λ_s) and strata thickness (λ_m) are known.

The average dip of the failure path is given by:

$$\beta = \alpha + \arctan\left\{\lambda_m/t_m + \lambda_m \tan\left[90^\circ - (\tau - \alpha)\right]\right\}$$

where α = dip angle of the bedding planes, τ = dip angle of the major joints, and $t_m = \lambda_s/\sin(\tau - \alpha)$.

Solving for β enables the average sliding surface from top to toe to be drawn. The angle of the steep joints, the average spacing between the steep joints, the stepped sliding path and the cliff face define the multiblock model (Figure 2) which is used to simulate the risk of sliding and toppling for the site. The simulation model of limiting equilibrium follows the solution of Hoek and Bray (1981) for a regular system of structural blocks.

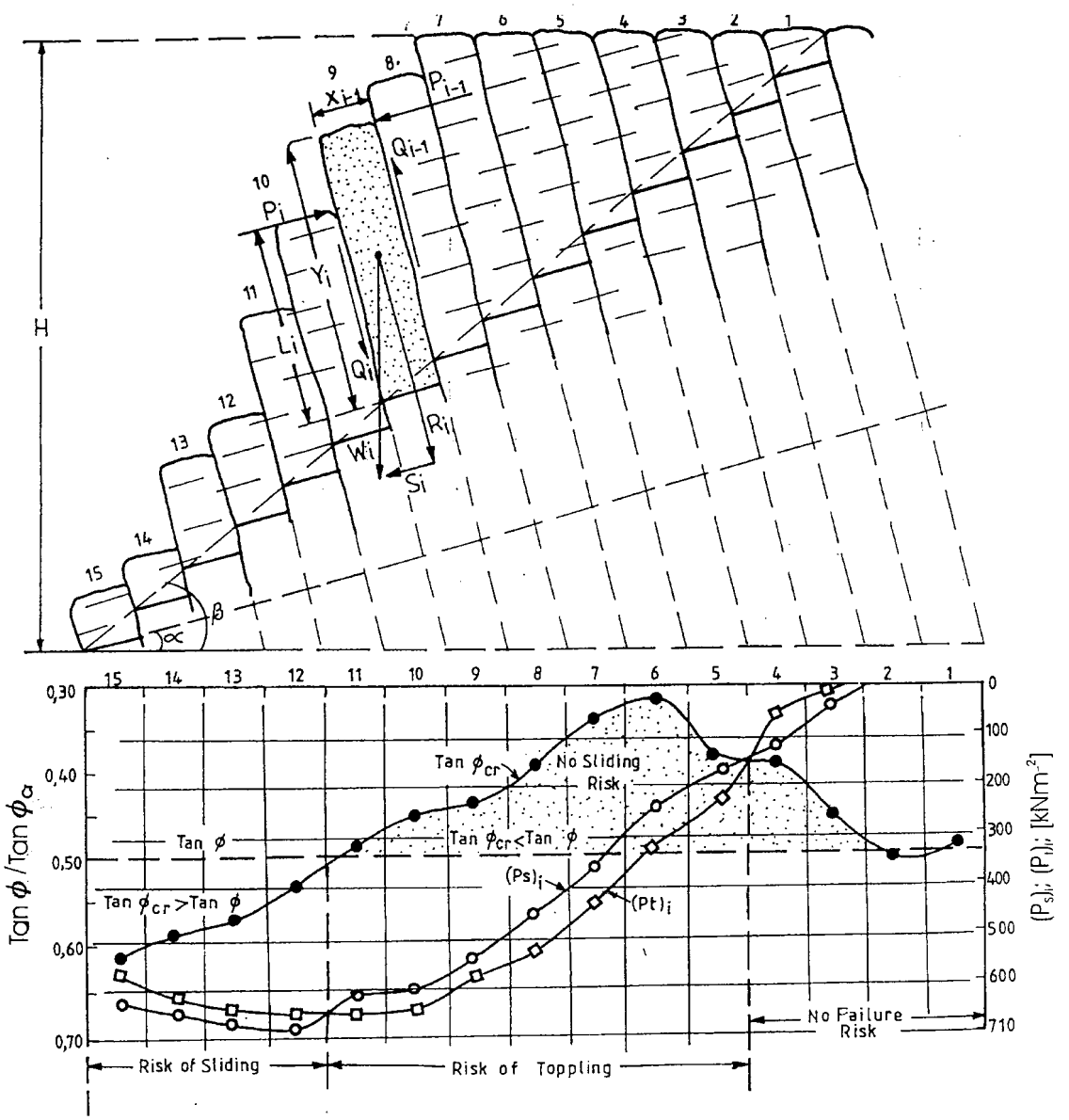

Figure 2. Multiblock model for cliff limiting equilibrium analysis using Druidston data (see text for explanation of symbols)

The height (Y_i) and width (X_i) of the individual block, the joint contact length (L_i) and laboratory-determined value of the joint friction angle (ϕ) are used to compute toppling forces $(P_t)_i$ and sliding forces $(P_s)_i$ for each block. The simulation programme follows Hoek and Bray's (1981) iterative approach to calculate toppling $(P_t)_i$ and $(P_s)_i$ forces for each block from the top to the base of the cliff.

The necessary forces to prevent toppling failure for each block are:

$$(P_t)_i = [(P_t)_{i-1}(Y_i - X_i \tan \varphi) + (W_i/2)(Y_i \sin \alpha - X_i \cos \alpha)]/L_i$$

and the forces preventing sliding failure are:

Table II. Computed values of toppling forces (P_t), sliding forces (P_s) and critical friction coefficients (tan ϕ_{crit}) for Druidston

Block no.	P_t (kN/m^{-2})	P_s (kN/m^{-2})	tanϕ_{crit}
1	0	0	0·48
2	0	0	0·51
3	23	43	0·47
4	76	115	0·41
5	214	157	0·39
6	335	238	0·31
7	437	358	0·34
8	521	459	0·40
9	585	541	0·44
10	630	603	0·45
11	655	647	0·47
12	659	670	0·53
13	642	663	0·57
14	603	654	0·58
15	541	610	0·62

Table III. Computed perpendicular forces (R), tangential forces (S) and available friction resistances (F_r at the base for Druidston

Block no.	R (kN/m^{-2})	S (kN/m^{-2})	F_r (kN/m^{-2})
1	73	48	55
2	220	172	166
3	335	244	252
4	461	330	347
5	588	418	442
6	298	179	221
7	283	179	213
8	272	178	205
9	262	178	197
10	251	178	189
11	241	178	182
12	224	168	168
13	231	192	174
14	176	133	133
15	246	239	185

$$(P_s)_i = (P_s)_{i-1} + [W_i(\tan \varphi \cos \alpha - \sin \alpha)]/(1 - \tan^2 \varphi)$$

Critical angles of the joint friction block are evaluated for each structural block as a function of perpendicular force R_i and tangential shearing force S_i.

R_i is the force induced by the weight (W_i) of the ith block on its base which is accepted as a downward vector, though it can be regarded as an upward vector when considering the reaction force at the base. The effect on the calculation of the friction resistance at the base of the block is the same.

The components R_i and S_i are evaluated by the following equations:

$$R_i = W_i \cos \alpha + [(P_t)_i - (P_s)_{i-1}] \tan \varphi$$

$$S_i = W_i \sin \alpha + [(P_t)_i - (P_s)_{i-1}]$$

Sample results for Druidston are shown in Tables II and III.

Whilst the model has the appearance of a back analysis because it admits a given sliding surface to evaluate the likely mobilized resistance values at particular cliff sites at failure, it can undertake direct analysis using a range of strength values and residual friction angles for the base of the blocks.

For a given site, the number and dimensions of the structural blocks are computed as functions of cliff

Table IV. Summary of engineering data for Druidston along joints and bedding planes

	⊥ Joints	// Bedding plane
Core reference	Z1	X1
Stress rate <V/s>*0·001	4	4
Core straightness (mm)	0·12	0·16
End parallelism (mm)	0·17	0·20
L/D ratio	2·00	2·00
Uniaxial compressive strength (field; MPa)	43·5 ± 10	57·97 ± 20
Uniaxial compressive strength (lab.; MPa)	49·7	54·0
Internal shear angle ϕ (deg.)	42·5	37
Cohesion (MPa)	11·88	17·4
Discontinuity shear angle ϕ_d (deg.)	37·76	57·09

height, distance from the cliff top to the occurrence point of the stepped sliding path and the average spacing between the steep joints. The competence of the model was checked using field and laboratory measurements as input variables from various sites, e.g. Druidston (Table IV).

SITE ANALYSIS

Locations within the Old Red Sandstone, Dinantian, Namurian and Westphalian (Figure 1) were selected for detailed analysis of engineering geology parameters, failure mechanisms and stability modelling. These rocks constitute >70 per cent of the coastal geological outcrops of the PCNP. Results from Druidston are shown fully in Table II which details computed values for sliding, toppling forces and critical coefficients, and Table III showing values obtained for perpendicular, tangential forces and available frictional resistance generated at the base of the structural blocks. A detailed limiting equilibrium analysis diagram is also presented for the multiblock numerical model (Figure 2). All other sites are discussed in outline only.

Druidston (Figures 1 and 3A, Tables I–IV)

Lower Westphalian and Lower Namurian sequences are exposed, consisting of sandstones, siltstones, shales and clays. At Druidston, siltstone bedding planes and steeply dipping joints intersect at 70°. The development of failure phenomena is facilitated by the existence of highly fissured and weathered clays/siltstones in the lower 15 m of the cliff base which are cut by two suites of principal subvertical joints. Within the 60° sloping cliff face major toppling and translational failures have occurred in the overlying well-bedded and jointed weathered sandstone rocks (B1 and J1, J2 and J3 in Figure 3A). A total of some 1500 m^3 of material is involved in the movements. Pressure release jointing and other weathering agents reduce interlock within the rock mass to form a series of detaching columns which are liable to failure as cliff undercutting takes place. The rocks of this section are variable in the details of their engineering geology parameters, and representative values are shown below:

Cliff height: 24–27 m
Cliff face azimuth: 165–345°
Dip angle of cliff face: 60°
Bulk unit weight: 2·41 Mg m^{-3}
Joint friction angle ϕ : 26°
Strike of bedding plane: 153–333°
Main bedding plane spacing: 2·2–2·5 m
Joint length: 10 m

Analysis suggests that the ratio between tan Φ available along a joint system and the critical value (tan Φ_{crit}) required for the condition or limiting equilibrium can be accepted as representative of safety factor values for each structural block. By successive iteration the model evaluates values of sliding forces (P_s) and toppling forces (P_t), and the critical friction coefficient (tan Φ_{crit}) for every block (Table II). Sliding forces (P_s) exceed toppling forces (P_t) and the tangential forces (S) are higher than the

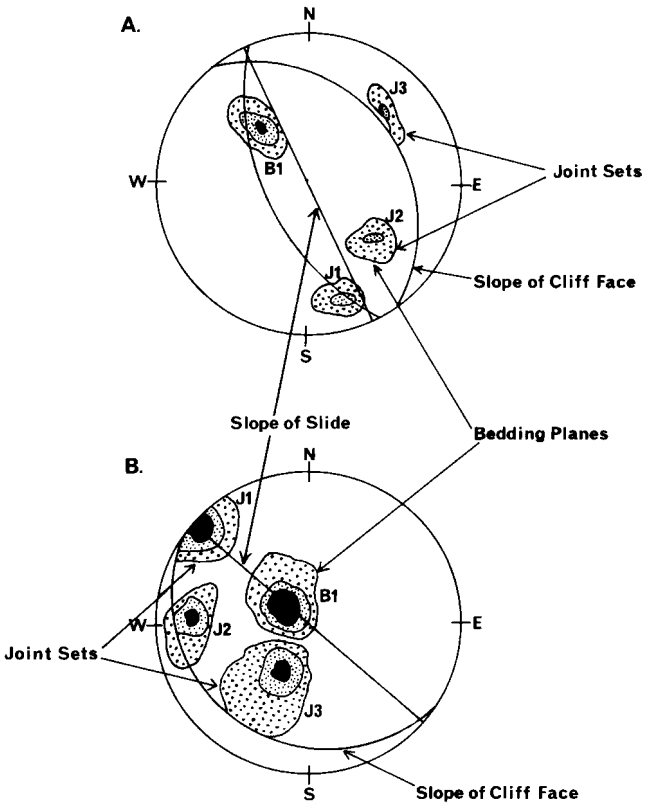

Figure 3. Stereonets of geological measurements at (A) Druidston and (B) St Govan's Head

frictional resistance available at the base of the lower structural blocks (Table III). Figure 2 illustrates the risk of sliding for the lower structural blocks where the critical coefficient for safety (tan Φ_{crit}) exceeds the available friction coefficient (tan Φ). In the upper part of the cliff, P_t forces exceed P_s forces (Figure 2), and there is a potential risk of local toppling of the structural blocks. This will be enhanced as structural loosening proceeds due to progressive movement of the lower block units.

St Govan's Head (Figures 1 and 3B, Tables I and V)

This is the easternmost headland of the southwest Dyfed coastline and consists of a Carboniferous Limestone (Dinantian) headland extending into the Outer Bristol Channel and open to southerly wave attack. The headland cliff slopes at 85° with abundant blocks forming a toe talus of about 130 m^3. These blocks are related to rockfalls from the B1 bedding planes and perpendicular J1, J2 and J3 joint sets (Figure 3B). Site investigation indicated that recession is achieved by high frequency, low magnitude rockfall events rather than from occasional, massive failures. Discontinuities are almost grid-like in occurrence with spacing decreasing in the upper cliff face and discontinuity opening reaching the moderately wide values (ISRM, 1981) of 5–10 mm. Engineering properties are summarized in Table V. Stability analysis using the numerical model suggests that the risk of translation failure is low. Similarly, the risk of toppling failure is limited where lateral forces within the discontinuities are small. However, where cliff base undercutting reaches 1·0 m, the stability factor reaches 1·0 and lateral forces in excess of 100 kN m^{-2} can produce similar reductions in the safety factor even in the absence of basal undercutting.

Table V. Summary of engineering data for St Govan's Head along joints and bedding planes

	⊥ Joints	// Bedding plane
Core reference	Z1	Y1
Stress rate <V/s>*0·001	3	3
Core straightness (mm)	0·17	0·18
End parallelism (mm)	0·13	0·17
L/D ratio	2·00	1·87
Uniaxial compressive strength (field; MPa)	50·08 ± 30	57·88 ± 30
Uniaxial compressive strength (lab.; MPa)	40·4	32·58
Internal shear angle ϕ (deg.)	48·8	50·74
Cohesion (MPa)	7·5	5·76
Discontinuity shear angle ϕ_d (deg.)	37·5	36·91

Mill Bay (Figure 1, Tables I and VI)

In the Milford Haven area, the Old Red Sandstone outcrops continuously for about 30 km, except for some short sections extending eastwards from Wooltack Point. Planar and wedge sliding were common, in the brittle rock strata and two main discontinuity patterns were found. Between the bedding planes, near-vertical discontinuities striking 55–235° and dipping 70° occurred. The well-marked joint pattern reduces interlock forces and produces good water drainage, and block failure occurs when the rock dip exceeds the friction angle of the blocks resting on that plane. Whilst the intact rock compressive strength was one of the highest recorded (Table VI), discontinuities are evidently a more critical control. There is a continuity within the major joints, and joint separation of some 3–5 mm has occurred. Numerical modelling suggested that with an overturning force of $> 500\,\mathrm{kN\,m^{-2}}$, the risk of translational failure is small, though toppling could occur with critical thrust forces $> 280\,\mathrm{kN\,m^{-2}}$. In reality, plane failure was found. This is the only occasion where such a discrepancy was found and further analysis is required to test the applicability of the model in areas of low translation and toppling risk.

Wisemans Bridge (Figure 1, Tables I and VII)

Tectonically disturbed bed sequences are found in the Lower Coal Measures (Westphalian) sandstones, shales and clays. Basal failure surfaces were propagated along bedding-plane contacts between porous friable sandstone and other rock types. Most soft-rock failures comprise wedge or

Table VI. Summary of engineering data for Mill Bay along joints and bedding planes

	⊥ Joints	// Bedding plane
Core reference	Z1	X1
Stress rate <V/s> *0·001	4	4
Core straightness (mm)	0·18	0·17
End parallelism (mm)	0·20	0·13
L/D ratio	2·00	2·00
Uniaxial compressive strength (field; MPa)	58·35 ± 30	57·84 ± 30
Uniaxial compressive strength (lab.; MPa)	76·08	64·39
Internal shear angle ϕ (deg.)	45·77	37·96
Cohesion (MPa)	15·5	15·72
Discontinuity shear angle ϕ_d (deg.)	44·0	43·98

Table VII. Summary of engineering data for Wiseman's Bridge

	⊥ Joints	// Bedding plane
Core reference	Z1	X1
Stress rate <V/s> *0·001	4	4
Core straightness (mm)	0·17	0·14
End parallelism (mm)	0·23	0·18
L/D ratio	2·00	2·00
Uniaxial compressive strength (field; MPa)	$61{\cdot}2 \pm 20$	$52{\cdot}0 \pm 20$
Uniaxial compressive strength (lab.; MPa)	53·2	48·6
Internal shear angle ϕ (deg.)	40·3	41·6
Cohesion (MPa)	28·4	27·5
Discontinuity shear angle ϕ_d (deg.)	50·49	50·22

rotational movements because of the variable lateral restraint provided by subvertical joints or faults and along which block release occurs. Post-failure deformation of most of these sequences has resulted in master joint development, typically parallel to the strike and dip directions of primary bedding planes. Uniaxial compressive strengths were similar to those found at Druidston (Table IV). The *JRC* calculated from back-substitution was comparable to a vertical roughness of 8·4. The high basic friction angle produced a residual angle of 40° which raised the discontinuity shear angles accordingly (Table VII). The shrinkage and swelling stresses associated with the interbedded shales seem more than sufficient to contribute to disintegration of the brittle sandstones, though more site monitoring and swelling/shrinkage tests are required to confirm this observation. Numerical analyses indicated that there is a higher risk of toppling rather than translation and once retrogressive failures have been initiated in these rock sequences the orientation of the rock mass discontinuities will control the pattern of subsequent failure.

CONCLUSIONS

A range of field and laboratory structural and geomorphological data for representative sites of the Pembrokeshire Coast National Park were integrated into a numerical model based on rock prisms delineated by major joints, tension fractures of varying depths behind the cliff face, and stepped failure surfaces.

At three of the four sites the model correctly predicted the most common failure modes:

- At Druidston, sliding forces exceeded toppling forces though the latter were enhanced as structural loosening occurred during slide generation. Translation failure was the most common mass movement type in the field.
- At St Govan's Head, the low risk of translation failure was correctly predicted. Toppling is the most common failure mode and is associated with basal undercut depths of $>1{\cdot}0$ m and/or lateral forces in excess of $100\,\mathrm{kN\,m^{-2}}$.
- At Wiseman's Bridge there was a similar greater risk of toppling failure and forces associated with shrinkage and swelling of interbedded shales seem to be an important contributory factor in the generation of this failure type.

These three sites showed field evidence in agreement with the predictions and analyses generated by the model.

- At Mill Bay, numerical analyses suggested that there was a low risk of translation and toppling. Field

evidence, however, indicated that some planar failures had occurred. This discrepancy between the results of the model and the field evidence requires further analysis to establish if the model has lower validity at sites with very low toppling and translation risk.

However, the overall sound agreement between field observations, laboratory analyses and numerical evaluation suggests that the approach has the potential to identify the type and risk of coastal cliff failure within most of the geological and other environmental controls identified within this paper. In addition, the technique has been utilized successfully for other rock types, e.g. Lias rocks in South Wales (Williams *et al.*, 1993; Davies *et al.*, 1991) and coastal Romania.

REFERENCES

Allen, J. R. L. 1965. 'Upper Old Red Sandstone (Farlovian) Paleogeography in South Wales and the Welsh Borderland', *J. Sedim. Petrol.* 167–195.

Bandis, S., Lumsden, A. C. and Barton, N. R. 1981. 'Experimental studies of scale effects on the shear behaviour of rock joints', *R. Mech., Min. Sci. Geomech. Abstr.*, **18**, 1–21.

Barton N. R. 1973. 'Review of a new shear strength criterion for rock joints', *Eng. Geol.*, **7**, 287–332.

Barton, N. R. and Choubey, A. W. 1977. 'The shear strength of rock joints in theory and practice', *Rock Mech.*, **10**, 1–54.

Carr, A. 1962. 'Cartographic record and historical accuracy, *Geography*, **47**(2), 215, 135–145.

Davies, P., Williams, A. T. and Bomboe, P. 1991. 'Numerical modelling of Lower Lias rock failure in the coastal cliffs of South Wales', in Kraus, N. C., Gingerlich, K. and Kreibel, D. L. (Eds), *Coastal Sediments 91*, **2**, 1599–1612.

Day, M. J. and Goudie, A. S. 1977. *Field Assessment of Rock Hardness using the Schmidt Test Hammer*. British Geomorphology Research Group Technical Bulletin **18**, 19–29.

Hoek, E. 1990. 'Strength of jointed rock masses', 23rd Rankine Lecture, *Geotechnique*, **33**(3), 187–223.

Hoek, E. and Bray, J. W. 1981. *Rock Slope Engineering*, Institute of Mining and Metallurgy, London, 309 pp.

Hoek, E. and Brown, E. T. 1988. 'The Hoek–Brown Failure Criterion – a 1988 update', *Rock Engineering for Undergroud Excavation*, Proc. 15th Canadian Rock Mechanics Symposium, University of Toronto, 31–38.

Hutchinson, J. N. 1988. 'General report: morphological and geotechnical parameters of landslides in relation to geology and hydrogeology', in Bonnard, C. (Ed.), Proc. 5th Int. Symposium on Landslides, 10–15 July 1988, Vol. 1, Balkema, Rotterdam.

ISRM (International Society for Rock Mechanics). 1981. *Rock Characterisation Testing and Monitoring, ISRM Suggested Methods*, (Ed. E. T. Brown), Pergamon Press, Oxford, 167 pp.

Jones, D. G. 1987. *The Stability of Coastal Cliffs along Sections of the Ceredigion Coastline*, PhD thesis, Polytechnic of Wales, 377 pp.

Jones, D. G. and Williams, A. T. 1991. 'Statistical analysis of factors influencing coastal erosion along a section of the West Wales coast, UK', *Earth Surf. Process. Landf.*, **16**(2), 95–112.

Jumikis, A. R. 1983. *Rock Mechanics*, 2nd edn, Gulf Publishing, London, 613 pp.

Kazi, A. and Al-Mansom, Z. R. 1980. 'Empirical relationship between Los Angeles abrasion and Schmidt hammer strength tests with application to aggregates around Jeddah' *Q. J. Eng. Geol.*, **13**, 45–52.

Komar, P. D. 1976. *Beach Processes and Sedimentation*, Prentice-Hall, Englewood Cliffs, NJ, 429 pp.

Miller, R. P. 1965. *Engineering Classification and Index Properties for Intact Rock*, PhD thesis, University of Illinois, 332 pp.

Patton, F. D. 1966. *Multiple Modes of Shear Failure in Rock and Related Materials*, PhD thesis, University of Illinois, 282 pp.

Scoble, M. J. and Leigh, W. J. P. 1982. 'Factors governing the stability of rock slopes in British surface coal mines', *Rock Mechanics*, AIME Proc. 23rd Symposium, 25–27 August, Berkeley, 1091–1099.

Terzaghi, K. 1962. 'Stability of steep slopes in hard, unweathered rock', *Geotechnique*, **12**, 251–270.

Williams, A. T. and Davies, P. 1987. 'Rates and mechanisms of coastal cliff erosion in Lower Lias rocks', in Kraus, N. C. (Ed.), *Coastal Sediments '87*, American Society of Civil Engineers, 1855–1870.

Williams, A. T., Davies, P. and Bomboe, P. 1993. 'Geometrical simulation studies of coastal cliff failures in South Wales, UK', *Earth Surf. Process. Landf.*, **18**, 703–720.

